# Nonreciprocity and the Optimum Operation of Ferrite Coupled Lines

Kang Xie, *Member, IEEE,* and Lionel E. Davis, *Fellow, IEEE*

***Abstract*—The first full-wave normal-mode analysis of ferrite coupled lines (FCL's) magnetized in the longitudinal direction is presented in this paper. It is found that the tangential and axial components of the guided electric and magnetic fields undergo a different change in the process of reversing the direction of magnetization. These changes cause the same input wave to decompose into the eigenmodes of the FCL differently for different direction of magnetization and, consequently, cause the nonreciprocal behavior of the magnetized FCL. A new optimum nonreciprocal operation condition is obtained, and applications to FCL circulators built on microstrips and striplines are discussed.**

***Index Terms*—Coupled transmission lines, ferrite circulators, ferrite devices.**

## I. Introduction

SINCE THE experimental discovery of ferrite coupled lines (FCL's) [1], several papers [2]–[5] have discussed the nonreciprocity in FCL's and the search for its optimum operation condition. Although the most promising potential applications are in distributed circulators for higher microwave frequencies, e.g., 60 GHz and above, devices operating at lower frequencies are discussed in this paper to demonstrate the behavior. Mazur and Mrozowski [2] used the coupled-mode method to show that the even and odd modes of a unmagnetized FCL become coupled when longitudinal magnetization is applied to the ferrite. They demonstrated that the behavior of a magnetized FCL was due to such coupling. They also found an optimum operation condition to be equal propagation constants for the unmagnetized FCL ($\beta_{\rm odd} = \beta_{\rm even}$). However, the $\beta_{\rm odd} = \beta_{\rm even}$ condition is not appropriate for a realistic design project because of the weak-coupling assumption intrinsic to all coupled mode theory. In 1995, Teoh and Davis [3] proposed a normal-mode approach. They explained the behavior of the magnetized FCL as the superposition of right- and left-hand-side elliptically polarized normal modes. They found that the phase difference between lines for normal mode one $(\phi_1)$ and normal mode two $(\phi_2)$ of the magnetized FCL is frequency dependent. For optimum operation, the normal mode equivalent to the $\beta_{\rm odd} = \beta_{\rm even}$ condition is $\phi_1 = -90°$, $\phi_2 = +90°$. It is this phase quadrature that is responsible for the nonreciprocal behavior of the magnetized FCL.

Manuscript received December 14, 1998. This work was supported by the Engineering and Physical Sciences Research Council, U.K., under Grant GR/L26445.

The authors are with the Department of Electrical Engineering and Electronics, University of Manchester Institute of Science and Technology, Manchester M60 1QD, U.K.

Publisher Item Identifier S 0018-9480(00)02775-7.

Subsequent experimental results confirmed both the coupled mode and normal mode understanding. However, neither of the experiments performed as well as might be expected. In Mazur's experiment [4], the measured isolation losses were 15–20 dB, insertion losses were 2.5–3 dB, and return losses were about 18 dB. Also, the Teoh *et al.* experiment [5] is not any better than Mazur's. A possible reason lies in the optimum condition of $-\phi_1 = \phi_2 = 90°$. Numerical calculation of the eigenmodes shows that the phase information is difficult to use because $\phi_1$ and $\phi_2$ are functions of space. The values of $\phi_1$ and $\phi_2$ also depend on which components of the electric (magnetic) field are used in the calculation so $\phi_1$ and $\phi_2$ cannot be uniquely defined. Consequently, the $-\phi_1 = \phi_2 = 90°$ condition cannot be relied upon to provide the optimum operation condition of the structure. The other possible reason lies in the assessment of the performance. Neither the coupled- nor normal-mode approach permits a full assessment of the performance of the magnetized FCL at either optimum operation condition ($\beta_{\rm odd} = \beta_{\rm even}$ or $-\phi_1 = \phi_2 = 90°$). Both theories neglect the internal structure of the guided mode and assume perfect power transfer between lines at the optimum operation point. It is shown below, however, that this assumption is not true. The power transfer reaches its maximum at these optimum operation points, but it is not necessarily 100%. It is necessary to determine the actual value of the power transfer coefficient of magnetized FCL's in order to select the best structure.

In this paper, the first full-wave normal-mode theory has been developed for the design of the FCL. By studying the energy flow carried by each line, a new normal-mode optimum operation condition is constructed through the integration of the $z$ component of the Poynting vector. Complete descriptions of the modes are obtained and all the information is retained within the optimum operation condition because both the imaginary and real parts of the electric and magnetic field enter the calculation through the integration. The arbitrariness of the use of $\phi_1$ and $\phi_2$ is, therefore, avoided. The new condition is based on a direct calculation of the power exchange ability of the two coupled lines in the magnetized FCL. Therefore, not only can the optimum operation point of a given FCL be found, a comparison of the optimum operation points of different FCL structures can also be made so that an overall best FCL can be identified.

It is well known that the propagation constant of a guided mode of a magnetized FCL is unchanged when the direction of the longitudinal magnetization reverses [6]. In this paper, we describe how the guided mode itself changes in the reversing process. Due to this change, the same input wave will be decomposed into the eigenmodes of the magnetized FCL differently for the different directions of magnetization. It is found that the

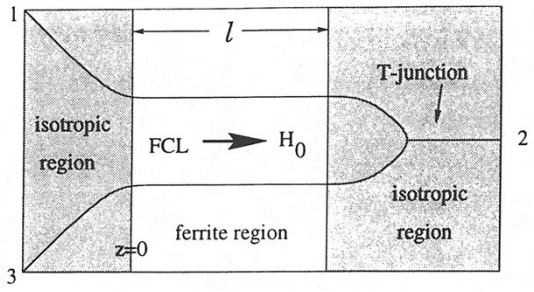


Fig. 1. Sketch of the proposed three-port distributed circulator.

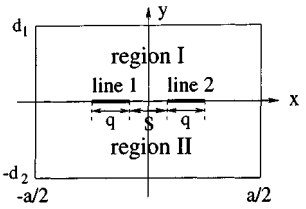


Fig. 2. Cross section of the FCL.

amplitude of the decomposition coefficient keeps constant, but a phase shift occurs with the reversal of the direction of magnetization on the FCL. It is this phase shift, plus the change in the eigenmode itself, that causes the magnetized FCL to behave in a nonreciprocal way. In this paper, we describe a way to incorporate these changes, and the nonreciprocal behavior of the magnetized FCL is finally realized through a simple sign change in an integration.

## II. Theory

The three-port distributed circulator comprising a magnetized FCL section in cascade with a T-junction, as shown in Fig. 1 (after Mazur [4]). The direction of the applied static magnetic field $H_0$ is arbitrary (parallel or antiparallel with respect to the direction of propagation), but it determines the direction of circulation. The main part of the distributed circulator is the FCL, which is uniform in the $z$-direction for a finite length $\ell$. The cross section of the FCL is sketched in Fig. 2. Region I (II) represents all the material above (below) the coupled lines. It can be multilayered structure and it can contain ferrite. Lines 1 and 2 represent the two coupled lines. They can be microstrips or striplines. The metal sidewalls and top walls are present for the convenience of the finite-element method (FEM), and they also serve to suppress radiation losses.

The expected behavior of the FCL is sketched in Fig. 3. When the signal enters port 1 in Fig. 1, the situation in the magnetized FCL is equivalent to Fig. 3(a) plus (b). An even signal will come out of the two arms of the FCL and add up to give an output at port 2 in Fig. 1. When the signal enters from port 2, it divides at the T-junction and enters the magnetized FCL evenly in a direction opposite to that of $H_0$. The situation resembles Fig. 3(c), and an output at port 3 in Fig. 1 is expected. When the signal enters port 3, the situation corresponds to Fig. 3(a) minus (b). The waves entering the T-junction are $\pi$ out of phase and cancel each other at port 2. The reflection enters the magnetized FCL as an odd mode and a situation like Fig. 3(d) is realized. The final output will be at port 1. Therefore, the expected circulation of

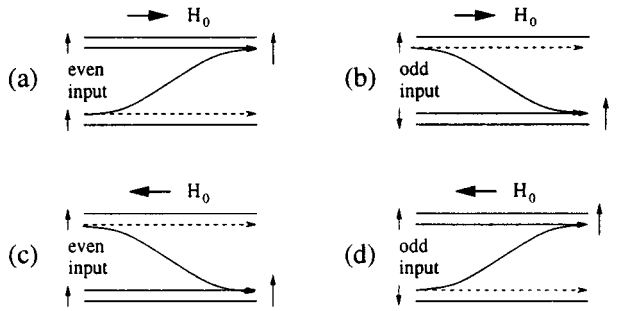


Fig. 3. Expected behavior of the FCL. The dashed line represents (unwanted) direct signal transfer.

the device is $1 \rightarrow 2 \rightarrow 3 \rightarrow 1$. If the magnetized FCL can perform each of the functions in Fig. 3 with 100% efficiency, the proposed device in Fig. 1 will behave as an ideal circulator. The determination of the length $\ell$ of the FCL, and its efficiency of power transfer, are the subjects of this paper.

As shown in Fig. 1, the ferrite has input and output interfaces with the isotropic media. Waves encountering these discontinuities will be scattered, thus, in reality, transmission and reflection coefficients at both interfaces need to be determined. In this paper, we are mostly interested in the power transfer between the two coupled lines and in determining the plane at which to extract the power guided by the lines to get the best result. To simplify the analysis, we have assumed that the FCL is of semiinfinite extent, thus, only the interface on the input side (the "first interface") needs to be taken into account. When a signal meets this interface, it decomposes into the eigenmodes of the magnetized FCL. The extraction of guided power introduces the second interface, and this will inevitably perturb the system. Our theoretical prediction is, therefore, only applicable to the experimental case when this perturbation is small. The perturbation can be minimized by designing the output section to matched the magnetized FCL section so that reflections at the second interface are negligible. The eigenmodes of the magnetized FCL will still be decomposed into eigenmodes of the waveguide of the output section at the second interface. However, since the reflection is negligible, this decomposition will cause no power to be redistributed among the two coupled lines, and the second interface can, therefore, effectively be neglected. The first interface needs to be analyzed in any case to obtain information on the eigenmodes propagating in the magnetized FCL. Such decomposition determines the behavior of the FCL. For an unmatched FCL, some amount of power will be reflected back into the FCL at the second interface. This reflected power will participate in the complex procedure happening there, but for simplicity, it is not included here. However, the inclusion of the discontinuities at both the input and output interfaces is necessary for a complete description of an FCL structure, and this will be the subject of a later paper. Experimental verification of the theory presented here is in hand, and will be published at a later date.

### A. Vectorial-Wave Equation

Maxwell's equations for time–harmonic waves are

$$\nabla \times \mathbf{E} = -j[\mu]\mu_0\omega\mathbf{H} \tag{1}$$

$$\nabla \times \mathbf{H} = +j[\varepsilon]\varepsilon_0\omega\mathbf{E} + \sigma\mathbf{E} \tag{2}$$

where a time variation of the form $e^{j\omega t}$ is assumed, and $\mathbf{E}$ is the electric field, $\mathbf{H}$ is the magnetic field, $\omega$ is the angular frequency, $\varepsilon_0$ and $\mu_0$ are, respectively, the permittivity and permeability of free space, $[\mu] \equiv [\mu(x,y)]$ is the relative permeability tensor, and $[\varepsilon] \equiv \varepsilon(x,y)$ is the scalar relative permittivity of the media in the coupled waveguides. Assuming uniform magnetization in the $z$-direction, $[\mu]$ is given, to a first order of approximation, by

$$[\mu] = \begin{bmatrix} \mu & +j\kappa & 0 \\ -j\kappa & \mu & 0 \\ 0 & 0 & 1 \end{bmatrix} \tag{3}$$

where $\mu = 1 + (\omega_0\omega_m/(\omega_0^2 - \omega^2))$, $\kappa = (\omega\omega_m/(\omega_0^2 - \omega^2))$, $\omega_m = \mu_0\gamma M_s$, and $\omega_0 = \mu_0\gamma H_0$. $\gamma$ is the gyromagnetic ratio that has a value of $1.759 \times 10^{11}$C/kg, $H_0$ is the bias field, and $M_s$ is the saturation magnetization.

Assuming perfect conductivity of the metal, all the metal surfaces can be treated as boundary conditions, and $\sigma$ is, therefore, zero everywhere in the field regions. The following vectorial wave equation can be derived from (1) and (2):

$$\nabla \times (\varepsilon^{-1}\nabla \times \mathbf{H}) - \frac{\omega^2}{c^2}[\mu]\mathbf{H} = 0 \tag{4}$$

where $c = 1/\sqrt{\varepsilon_0\mu_0}$ is speed of light in vacuum. Since the waveguide is uniform in the $z$-direction, all field components will have a $z$ dependence of $e^{-j\beta z}$ where $\beta$ is the propagation constant. Equation (4) can be cast into Konrad's functional [7] and can be solved using the FEM [8], [9] to obtain the propagation constant $\beta$ and the modal field patterns $\mathbf{H}(x,y)$. $\mathbf{E}(x,y)$ are obtainable from $\mathbf{H}(x,y)$ by using (2).

The guided modes of the magnetized FCL always contain regions of elliptical polarization, and the power transfer effect can be explained in terms of the superposition of these elliptically polarized modes. To obtain good nonreciprocal behavior, the number of modes should be limited to two, which are denoted by $[\mathbf{E}_1(x,y), \mathbf{H}_1(x,y)]$, $\beta_1$, and $[\mathbf{E}_2(x,y), \mathbf{H}_2(x,y)]$, $\beta_2$, where $\beta_1 > \beta_2$. The even and odd modes at the input in the isotropic region are denoted by $[\mathbf{E}_e(x,y), \mathbf{H}_e(x,y)]$, $\beta_e$, and $[\mathbf{E}_o(x,y), \mathbf{H}_o(x,y)]$, $\beta_o$, respectively, where even (odd) mode is defined as having the electric field $E_y$, an even (odd) function with respect to the $x = 0$ plane. The input modes can be delivered from any kind of compatible waveguide. From these modal fields, the integration

$$P_{mn} = \int_{-\infty}^{\infty} dy \int_{-\infty}^{\infty} dx \left( E_{mx}H_{ny}^* - E_{my}H_{nx}^* \right) \tag{5}$$

can be computed, where $m, n = 1, 2, e, o$. Also, $P_{mnr}$ ($P_{mnl}$) is defined as the integration over the right- (left-)-hand side of the waveguide cross section. The orthogonality of these modes implies that $P_{12} = P_{21} = P_{eo} = P_{oe} = 0$. However, $P_{1e}$, $P_{e1}$, $P_{1o}$, $P_{o1}$, $P_{2e}$, $P_{e2}$, $P_{2o}$, and $P_{o2}$ are not zero, nor are $P_{mnr}$ and $P_{mnl}$.

### B. Decomposition of the Input Mode at the FCL Interface

At the first interface, where the input waveguide meets the magnetized FCL (see Fig. 1), the input wave is decomposed into the eigenmodes of the FCL. This process can be treated using the modal analysis method [10].

Suppose the input wave consists of $B_e$ of the even mode and $B_o$ of the odd mode, i.e., $B_e[\mathbf{E}_e, \mathbf{H}_e] + B_o[\mathbf{E}_o, \mathbf{H}_o]$, where $B_o$ and $B_e$ are the complex amplitudes. The reflection from the FCL is $A_e[\mathbf{E}_e, -\mathbf{H}_e] + A_o[\mathbf{E}_o, -\mathbf{H}_o]$, plus higher order modes. The transmitted wave is $\sum_{n=1}^{\infty} A_n[\mathbf{E}_n, \mathbf{H}_n]$. Boundary conditions at the interface are the continuity of all the tangential-field components. Both guided modes and evanescent modes should be included in the boundary conditions in principle, but inclusion of all the guided modes is often enough to give a good answer in practice. In the current problem, to obtain good nonreciprocal effects, we design the waveguide so that only two elliptically polarized modes can propagate in the magnetized FCL. Also, we assume that the input waveguide can support only two modes, the even and odd modes. Imposing the boundary conditions at $z = 0$ gives

$$\begin{aligned} &B_oE_{ox} + B_eE_{ex} + A_oE_{ox} + A_eE_{ex} \\ &\quad = A_1E_{1x} + A_2E_{2x} \end{aligned} \tag{6}$$

$$\begin{aligned} &B_oE_{oy} + B_eE_{ey} + A_oE_{oy} + A_eE_{ey} \\ &\quad = A_1E_{1y} + A_2E_{2y} \end{aligned} \tag{7}$$

$$\begin{aligned} &B_oH_{ox} + B_eH_{ex} - A_oH_{ox} - A_eH_{ex} \\ &\quad = A_1H_{1x} + A_2H_{2x} \end{aligned} \tag{8}$$

$$\begin{aligned} &B_oH_{oy} + B_eH_{ey} - A_oH_{oy} - A_eH_{ey} \\ &\quad = A_1H_{1y} + A_2H_{2y}. \end{aligned} \tag{9}$$

By multiplying (6) with $H_{ey}^*$, and (7) with $H_{ex}^*$, and then integrating their subtraction over the cross section of the waveguide, we get

$$P_{ee}B_e + P_{ee}A_e = P_{1e}A_1 + P_{2e}A_2 \tag{10}$$

where $P_{ee}$, $P_{1e}$, and $P_{2e}$ are integration coefficients defined in (5). The orthogonality of modes has been used in deriving (10). Further manipulation on the boundary conditions, i.e., (6)–(9), in a similar way generates three more equations for the reflection coefficients $A_e$, $A_o$, and the transmission coefficients $A_1$ and $A_2$. The four equations can then be written in the following matrix form $[P][A] = [B]$:

$$\begin{bmatrix} P_{1o} & P_{2o} & -P_{oo} & 0 \\ P_{1e} & P_{2e} & 0 & -P_{ee} \\ P_{11}^* & 0 & P_{1o}^* & P_{1e}^* \\ 0 & P_{22}^* & P_{2o}^* & P_{2e}^* \end{bmatrix} \begin{bmatrix} A_1 \\ A_2 \\ A_o \\ A_e \end{bmatrix} = \begin{bmatrix} P_{oo}B_o \\ P_{ee}B_e \\ P_{1o}^*B_o + P_{1e}^*B_e \\ P_{2o}^*B_o + P_{2e}^*B_e \end{bmatrix}. \tag{11}$$

### C. Power Flow in FCL

Any given input will decompose into $A_1$ of mode 1 and $A_2$ of mode 2 of the magnetized FCL, where $A_1$ and $A_2$ are obtained from $[A] = [P]^{-1}[B]$. The field propagating in the FCL is, therefore,

$$\begin{aligned} E_x &= A_1E_{1x}e^{-j\beta_1 z} + A_2E_{2x}e^{-j\beta_2 z} \\ E_y &= A_1E_{1y}e^{-j\beta_1 z} + A_2E_{2y}e^{-j\beta_2 z} \\ H_x &= A_1H_{1x}e^{-j\beta_1 z} + A_2H_{2x}e^{-j\beta_2 z} \\ H_y &= A_1H_{1y}e^{-j\beta_1 z} + A_2H_{2y}e^{-j\beta_2 z}. \end{aligned}$$

The $z$ component of the Poynting vector is

$$\begin{aligned}S_z &= \frac{1}{2}\operatorname{Re}\Big(E_x H_y^* - E_y H_x^*\Big)\\ &= \frac{1}{2}|A_1|^2\operatorname{Re}\Big(E_{1x}H_{1y}^* - E_{1y}H_{1x}^*\Big)\\ &\quad + \frac{1}{2}|A_2|^2\operatorname{Re}\Big(E_{2x}H_{2y}^* - E_{2y}H_{2x}^*\Big)\\ &\quad + \bigg[\frac{1}{2}\operatorname{Re}\Big(A_1A_2^*\Big)\operatorname{Re}\Big(E_{1x}H_{2y}^* - E_{1y}H_{2x}^*\Big)\\ &\qquad - \frac{1}{2}\operatorname{Im}\Big(A_1A_2^*\Big)\operatorname{Im}\Big(E_{1x}H_{2y}^* - E_{1y}H_{2x}^*\Big)\bigg]\\ &\quad \times\cos\Big[(\beta_1-\beta_2)z\Big]\\ &\quad + \bigg[\frac{1}{2}\operatorname{Re}\Big(A_1A_2^*\Big)\operatorname{Im}\Big(E_{1x}H_{2y}^* - E_{1y}H_{2x}^*\Big)\\ &\qquad + \frac{1}{2}\operatorname{Im}\Big(A_1A_2^*\Big)\operatorname{Re}\Big(E_{1x}H_{2y}^* - E_{1y}H_{2x}^*\Big)\bigg]\\ &\quad \times\sin\Big[(\beta_1-\beta_2)z\Big]\\ &\quad + \bigg[\frac{1}{2}\operatorname{Re}\Big(A_1A_2^*\Big)\operatorname{Re}\Big(E_{2x}H_{1y}^* - E_{2y}H_{1x}^*\Big)\\ &\qquad + \frac{1}{2}\operatorname{Im}\Big(A_1A_2^*\Big)\operatorname{Im}\Big(E_{2x}H_{1y}^* - E_{2y}H_{1x}^*\Big)\bigg]\\ &\quad \times\cos\Big[(\beta_1-\beta_2)z\Big]\\ &\quad - \bigg[\frac{1}{2}\operatorname{Re}\Big(A_1A_2^*\Big)\operatorname{Im}\Big(E_{2x}H_{1y}^* - E_{2y}H_{1x}^*\Big)\\ &\qquad - \frac{1}{2}\operatorname{Im}\Big(A_1A_2^*\Big)\operatorname{Re}\Big(E_{2x}H_{1y}^* - E_{2y}H_{1x}^*\Big)\bigg]\\ &\quad \times\sin\Big[(\beta_1-\beta_2)z\Big] \qquad (12)\end{aligned}$$

The waveguide is enclosed in a metal tube, thus, there is no net power flow in the $x$- or $y$-direction. The power passing through any cross section $\mathbf{\Omega}$ of the magnetized FCL at distance $z$ is

$$\begin{aligned}W(z) &= \iint \mathbf{S}\cdot d\mathbf{\Omega}\\ &= \frac{1}{2}|A_1|^2\operatorname{Re}(P_{11}) + \frac{1}{2}|A_2|^2\operatorname{Re}(P_{22}) \qquad (13)\end{aligned}$$

where $(1/2)|A_1|^2\operatorname{Re}(P_{11})$ is the power carried by mode 1, and $(1/2)|A_2|^2\operatorname{Re}(P_{22})$ is the power carried by mode 2. Mode orthogonality ensures that no power is carried in between the two modes. Since no power can escape from the metal enclosure, and no loss is included in the calculation, $W$ is not a function of $z$.

The FCL contains two coupled lines. In the problem under consideration, the cross section of the FCL is always symmetric about $x = 0$, as shown in Fig. 2. It is, therefore, sensible to associate all power in the $x < 0$ region with the left-hand-side line (the "left line"), and all power in the $x > 0$ region with the right-hand-side line (the "right line"). The power carried by the right line is

$$\begin{aligned}W_r(z) &= \int_{-d_2}^{d_1} dy \int_0^{a/2} dx\, S_z\\ &= \frac{1}{2}|A_1|^2\operatorname{Re}(P_{11r}) + \frac{1}{2}|A_2|^2\operatorname{Re}(P_{22r})\\ &\quad + \frac{1}{2}\operatorname{Re}(A_1A_2^*P_{12r} + A_1^*A_2P_{21r})\cos\Big[(\beta_1-\beta_2)z\Big]\\ &\quad + \frac{1}{2}\operatorname{Im}(A_1A_2^*P_{12r} - A_1^*A_2P_{21r})\sin\Big[(\beta_1-\beta_2)z\Big]. \qquad (14)\end{aligned}$$

The power carried by the left line is obtainable from the above expression by replacing $P_{11r}$, $P_{22r}$, $P_{12r}$, and $P_{21r}$ with $P_{11l}$, $P_{22l}$, $P_{12l}$, and $P_{21l}$, respectively. It can be seen that power is periodically transferring between the two lines. The periodicity of the power transfer is

$$Z = \frac{2\pi}{|\beta_1-\beta_2|}. \qquad (15)$$

The power reflected back to the isotropic dielectric region can be calculated by using $A_o$ and $A_e$. For example, the power reflected back to the right line is

$$\begin{aligned}W_r^b(z) &= \frac{1}{2}|A_o|^2\operatorname{Re}(P_{oor}) + \frac{1}{2}|A_e|^2\operatorname{Re}(P_{eer})\\ &\quad + \frac{1}{2}\operatorname{Re}(A_oA_e^*P_{oer} + A_o^*A_eP_{eor})\cos\Big[(\beta_o-\beta_e)z\Big]\\ &\quad - \frac{1}{2}\operatorname{Im}(A_oA_e^*P_{oer} - A_o^*A_eP_{eor})\sin\Big[(\beta_o-\beta_e)z\Big]. \qquad (16)\end{aligned}$$

Similar expressions hold for the power reflected back to the left line of the dielectric waveguide.

TABLE I
EFFECTS OF REVERSING $H_0\hat{z}$ ON THE EIGENMODE OF A MAGNETIZED FCL

| | | |
|---|---|---|
| magnetization | $H_0\hat{z}$ | $-H_0\hat{z}$ |
| permeability tensor | $[\mu]$ | $[\mu]^*$ |
| propagation constant | $\beta$ | $\beta$ |
| transverse components | $(E_x, E_y, H_x, H_y)$ | $(E_x^*, E_y^*, H_x^*, H_y^*)e^{-j\theta}$ |
| longitudinal components | $(E_z, H_z)$ | $-(E_z^*, H_z^*)e^{-j\theta}$ |

### D. Bidirectionality and Nonreciprocity

When the direction of the magnetization $H_0\hat{z}$ is reversed, the propagation constants $\beta_1$ and $\beta_2$ will not change accordingly. This is the well-known bidirectionality theorem [6]. However, the guided modal field patterns $\mathbf{H}(x,y)$ and $\mathbf{E}(x,y)$ will change. The change in the modal patterns is the origin of the nonreciprocal power transfer effects in the magnetized FCL device.

*1) Effects of Reversing $H_0$ on the Decomposition Coefficients:* As shown in the Appendix A, the guided modal fields $\mathbf{H}(x,y)$ and $\mathbf{E}(x,y)$ change according to Table I when the direction of the magnetization $H_0\hat{z}$ is reversed. If the waveguide does not contain ferrite, i.e., $\kappa = 0$ everywhere, the change in

$H_0\hat{z}$ makes no difference to the waveguide and the eigenmode of a dielectric waveguide, therefore, has the following property:

$$\Big[E_t(x,y),E_z(x,y),H_t(x,y),H_z(x,y)\Big] = \Big[E_t^*(x,y),-E_z^*(x,y),H_t^*(x,y),-H_z^*(x,y)\Big]e^{-j\theta}. \tag{17}$$

Applying (17) and Table I to (5), the relationships of (18), shown at the bottom of this page, can be established for the procedure $H_0 \Rightarrow -H_0$ where $\theta_e$, $\theta_o$, $\theta_1$, and $\theta_2$ are the phase shifts associated with the even and odd modes of the input, and the first and second elliptically polarized modes of the magnetized FCL, respectively. $P_{eor}$, $P_{eol}$, $P_{oer}$, and $P_{oel}$ do not change in the procedure. $P_{ee}$, $P_{oo}$ can also be proved to be real by the use of (17) since

$$\begin{aligned} P_{ee} &= \int dy \int dx\Big(E_{ex}H_{ey}^* - E_{ey}H_{ex}^*\Big) \\ &= \int dy \int dx\Big(E_{ex}^* e^{-j\theta_e}H_{ey}e^{j\theta_e} - E_{ey}^* e^{-j\theta_e}H_{ex}e^{j\theta_e}\Big) \\ &= P_{ee}^*. \end{aligned} \tag{19}$$

Similarly, it can be shown that $P_{oo} = P_{oo}^*$. On the other hand, $P_{eor} = P_{eor}^* e^{-j\theta_e+j\theta_o}$, $P_{eol} = P_{eol}^* e^{-j\theta_e+j\theta_o}$, $P_{oer} = P_{oer}^* e^{j\theta_e-j\theta_o}$, and $P_{oel} = P_{oel}^* e^{j\theta_e-j\theta_o}$ are complex.

Since the eigenmodes of the magnetized FCL are changed, the same input wave will be decomposed differently for $H_0\hat{z}$ and $-H_0\hat{z}$ magnetization. This change is reflected in the reflection and transmission coefficient $[A]$. For a pure odd input, $B_e = 0$, $B_o = |B_o|e^{j\psi_o}$, where $\psi_o$ is the phase of $B_o$. From (11) and (18), one can see that if $[A] = [A_1, A_2, A_o, A_e]^T$ are the decomposition coefficients (transmission and reflection coefficients) for magnetization $H_0\hat{z}$, where the superscript "$T$" denotes transpose, then $\big[A_1^* e^{j(2\psi_o-\theta_o+\theta_1)}$, $A_2^* e^{j(2\psi_o-\theta_o+\theta_2)}$, $A_o^* e^{j2\psi_o}$, $A_e^* e^{j(2\psi_o-\theta_o+\theta_e)}\big]^T$ will be the decomposition coefficients for a $-H_0\hat{z}$ magnetization. It is interesting to note that the change is a pure phase shift. The amplitudes of the transmission and reflection coefficients are unchanged. Similarly, for a pure even input, $B_o = 0$, $B_e = |B_e|e^{j\psi_e}$, $[A]$ changes from $[A_1, A_2, A_o, A_e]^T$ to $[A_1^* e^{j(2\psi_e-\theta_e+\theta_1)}$, $A_2^* e^{j(2\psi_e-\theta_e+\theta_2)}$, $A_o^* e^{j(2\psi_e-\theta_e+\theta_o)}$, $A_e^* e^{j2\psi_e}]^T$ when the direction of magnetization is reversed. These changes are summarized in Table II.

*2) Effects of Reversing $H_0$ on the Power Flow:* The power flow associated with the right line is given in (14). When the magnetization is reversed, it can be seen from (18) and Table II

TABLE II
EFFECTS OF REVERSING $H_0\hat{z}$ ON THE REFLECTION AND TRANSMISSION COEFFICIENTS

| | $H_0\hat{z}$ magnetization | -$H_0\hat{z}$ magnetization |
|---|---|---|
| odd input | $A_1$ | $A_1^* e^{j(2\psi_o-\theta_o+\theta_1)}$ |
| | $A_2$ | $A_2^* e^{j(2\psi_o-\theta_o+\theta_2)}$ |
| | $A_o$ | $A_o^* e^{j2\psi_o}$ |
| | $A_e$ | $A_e^* e^{j(2\psi_o-\theta_o+\theta_e)}$ |
| even input | $A_1$ | $A_1^* e^{j(2\psi_e-\theta_e+\theta_1)}$ |
| | $A_2$ | $A_2^* e^{j(2\psi_e-\theta_e+\theta_2)}$ |
| | $A_o$ | $A_o^* e^{j(2\psi_e-\theta_e+\theta_o)}$ |
| | $A_e$ | $A_e^* e^{j2\psi_e}$ |

that the following changes occur for either a pure even or a pure odd input:

$$\begin{array}{ll} |A_1|^2P_{11r} \Rightarrow |A_1|^2P_{11r}^* & |A_2|^2P_{22r} \Rightarrow |A_2|^2P_{22r}^* \\ |A_1|^2P_{11l} \Rightarrow |A_1|^2P_{11l}^* & |A_2|^2P_{22l} \Rightarrow |A_2|^2P_{22l}^* \\ A_1A_2^*P_{12r} \Rightarrow A_1^*A_2P_{12r}^* & A_1^*A_2P_{21r} \Rightarrow A_1A_2^*P_{21r}^* \\ A_1A_2^*P_{12l} \Rightarrow A_1^*A_2P_{12l}^* & A_1^*A_2P_{21l} \Rightarrow A_1A_2^*P_{21l}^*. \end{array} \tag{20}$$

Using (20) in (14), it can be found that the first two terms and the term containing $\cos[(\beta_1-\beta_2)z]$ are invariable, while the term containing $\sin[(\beta_1-\beta_2)z]$ changes sign, which is responsible for the nonreciprocal behavior of the FCL.

For symmetrically placed coupled strips, $\mathrm{Re}(P_{11r})$ and $\mathrm{Re}(P_{22r})$ are generally not equal to $\mathrm{Re}(P_{11l})$ and $\mathrm{Re}(P_{22l})$, unless, as shown in Appendix B, the FCL is symmetrical in both $x$- and $y$-directions, and its ferrites in regions I and II are the same material, but magnetized in the opposite direction [see (39)]. For this special dually magnetized FCL, it can also be proven that in (14), the coefficient in front of $\cos[(\beta_1-\beta_2)z]$ is zero [see (46)] so that (14) reduces, for $H_0\hat{z}$ and $-H_0\hat{z}$, respectively, to

$$\begin{aligned} W_r^{+H_0} &= w + w_s \sin\Big[(\beta_1-\beta_2)z\Big] \\ W_l^{+H_0} &= w - w_s \sin\Big[(\beta_1-\beta_2)z\Big] \end{aligned} \tag{21}$$

$$\begin{aligned} W_r^{-H_0} &= w - w_s \sin\Big[(\beta_1-\beta_2)z\Big] \\ W_l^{-H_0} &= w + w_s \sin\Big[(\beta_1-\beta_2)z\Big] \end{aligned} \tag{22}$$

where

$$2w = \frac{1}{2}|A_1|^2\,\mathrm{Re}(P_{11}) + \frac{1}{2}|A_2|^2\,\mathrm{Re}(P_{22})$$

is the total power flowing in the magnetized FCL, and

$$w_s = \frac{1}{2}\,\mathrm{Im}\Big(A_1A_2^*P_{12r} - A_1^*A_2P_{21r}\Big).$$

Nonreciprocity is clearly demonstrated. It should be noted that the orthogonality condition $P_{12r} = -P_{12l}$ and $P_{21r} = -P_{21l}$ has been used in obtaining the power flow expressions of the

$$\begin{array}{llll} P_{11} \to P_{11}^* & P_{22} \to P_{22}^* & P_{ee} \to P_{ee} & P_{oo} \to P_{oo} \\ P_{1e} \to P_{1e}^* e^{j(\theta_e-\theta_1)} & P_{2e} \to P_{2e}^* e^{j(\theta_e-\theta_2)} & P_{1o} \to P_{1o}^* e^{j(\theta_o-\theta_1)} & P_{2o} \to P_{2o}^* e^{j(\theta_o-\theta_2)} \\ P_{11r} \to P_{11r}^* & P_{22r} \to P_{22r}^* & P_{11l} \to P_{11l}^* & P_{22l} \to P_{22l}^* \\ P_{12r} \to P_{12r}^* e^{j(\theta_2-\theta_1)} & P_{21r} \to P_{21r}^* e^{j(\theta_1-\theta_2)} & P_{12l} \to P_{12l}^* e^{j(\theta_2-\theta_1)} & P_{21l} \to P_{21l}^* e^{j(\theta_1-\theta_2)} \end{array} \tag{18}$$

left line. The required length of the dually magnetized FCL to obtain the largest nonreciprocal effect is

$$L = \frac{\pi}{2}\frac{1}{|\beta_1 - \beta_2|} \tag{23}$$

Similar analysis reveals that the reflected power also has nonreciprocal behavior.

For FCL structures other than this special type, (14) takes a more complicated form. The power carried on the right line for $H_0\hat{z}$, e.g., is

$$W_r^{+H_0} = w + w_s \sin\Big[(\beta_1 - \beta_2)z\Big] + \triangle w + w_c \cos\Big[(\beta_1 - \beta_2)z\Big] \tag{24}$$

where

$$\triangle w = \frac{1}{4}|A_1|^2 \operatorname{Re}(P_{11r} - P_{11l}) + \frac{1}{4}|A_2|^2 \operatorname{Re}(P_{22r} - P_{22l}) \neq 0$$

$$w_c = \frac{1}{2}\operatorname{Re}\Big(A_1 A_2^* P_{12r} + A_1^* A_2 P_{21r}\Big) \neq 0.$$

Since neither $\triangle w$ nor $w_c$ changes sign when the direction of magnetization is reversed, the magnetized FCL is not completely nonreciprocal. $w_c$ represents a reciprocal power transfer behavior, while $\triangle w$ causes no power to switch, but reduces the maximum power the two lines can exchange. Since, by definition, both $W_r$ and $W_l$ are positive quantities, it follows that $\sqrt{w_s^2 + w_c^2} \leq w - |\triangle w|$.

In this paper, we concentrate on FCL's whose two coupled lines are of equal width and zero thickness and symmetrically placed in the structure, as shown in Fig. 2. For such an FCL, $(\triangle w/w)$ and $(w_c/w)$ are very close to zero. In all the following numerical calculations, $\triangle w$ and $w_c$ are less than 1% of $w$. Such an FCL can basically be regarded as a nonreciprocal device, and (21), (22), and (23) are good descriptions of its behavior.

*3) Optimum Operation Condition:* For optimum nonreciprocal operation of a magnetized FCL, the ratio

$$\frac{w_s}{w} = 2\frac{\operatorname{Im}\Big(A_1 A_2^* P_{12r} - A_1^* A_2 P_{21r}\Big)}{\operatorname{Re}\Big(|A_1|^2 P_{11} + |A_2|^2 P_{22}\Big)} \tag{25}$$

has to be tuned to its maximum value. This is the new normal-mode equivalent to the $-\phi_1 = \phi_2 = 90^\circ$ condition of [3]. Compared with the old normal-mode condition, the new normal-mode condition gives a better prediction of the performance of the magnetized FCL because it allows a variation of the phase with position. Both the real and imaginary parts of the $\mathbf{E}$ and $\mathbf{H}$ field entered the calculation through (5), while in the old normal-mode optimum condition, the phases are assumed to be constants on the two coupled lines and jump abruptly from one value of line 1 to the other value of line 2. It is also better than the $\beta_{\text{even}} = \beta_{\text{odd}}$ condition of [2] in the sense that no weak coupling assumption is made in its derivation. It can, therefore, be applied to any structure with strong magnetization or strong coupling.

The ratio $(w_s/w)$ is usually close to, but less than, one at maximum. This means that a particularly magnetized FCL may not perform well even if we find the maximum value of $(w_s/w)$ for the structure. This is contrary to the result of the coupled mode theory, and the old normal-mode theory, where perfect operation is predicted once the condition $\beta_{\text{even}} = \beta_{\text{odd}}$ or $-\phi_1 = \phi_2 = 90^\circ$ is achieved.

## III. Numerical Results—Comparisons with Literature

In order to compare our numerical results with those experimental results that exist in the literature, it is necessary to convert the power transfer factor $(w_s/w)$ into the experimentally measurable quantities insertion loss and isolation, assuming the losses in the magnetized FCL and T-junction are negligible. For a signal entering from port 2, an even input mode will be excited, with power $(1/2)|B_e|^2 \operatorname{Re}(P_{ee}) \simeq 2w$. The power emerging from ports 1 and 3 is given by (21) and (22). These outputs correspond to

$$\text{insertion loss} = 10\log\left[\frac{1}{2} + \frac{1}{2}\frac{|w_s|}{w}\sin\left(\frac{\pi}{2}\frac{\ell}{L}\right)\right] \tag{26}$$

$$\text{isolation} = 10\log\left[\frac{1}{2} - \frac{1}{2}\frac{|w_s|}{w}\sin\left(\frac{\pi}{2}\frac{\ell}{L}\right)\right] \tag{27}$$

where $\ell$ is the actual length of the magnetized FCL and $L = (\pi/2)(1/|\beta_1 - \beta_2|)$ is the required length. It should be noted that $L$ is function of frequency, while $\ell$ is a constant. The situation with signal entering from ports 1 or 3 is more complicated, but the performance is expected to be at the same level.

The return loss can be estimated from (16). For an even input, it is found that the reflection coefficient of the even mode is much bigger than that of the odd mode, i.e., $|A_e| \gg |A_o|$. The reflected power levels are, therefore, $W_r^{(b)} \simeq (1/2)|A_e|^2 \operatorname{Re}(P_{eer})$ and $W_l^{(b)} \simeq (1/2)|A_e|^2 \operatorname{Re}(P_{eel})$, which add up at port 2 to give $2w^{(b)} = (1/2)|A_e|^2 \operatorname{Re}(P_{ee})$. The return loss is, therefore,

$$\text{return loss} = 10\log\left(\frac{w^{(b)}}{w}\right) = 20\log\left(\frac{|A_e|}{|B_e|}\right). \tag{28}$$

As expected, the return loss is directly related to the (normalized) reflection coefficient.

The coupled slotline structure analyzed by Mazur for its "basis guide" even and odd modes (see [4, Fig. 3]) has been reexamined. Using Fig. 2 to represent Mazur's structure, then region I is air and region II consists of three layers: the first layer beneath the coupled slotlines is a 0.127-mm-thick dielectric film with $\varepsilon_d = 2.22$, the second layer is a 0.5-mm ferrite slab with $\varepsilon_f = 13.5$, and the third layer is again air. Other dimensions in our notation are $d_1 = d_2 = 3.6$ mm, $a = 1.7$ mm, and $q = s = 0.5$ mm. The ferrite is just saturated $(H_0 = 0)$ with $M_s = 340$ kA/m. Mazur found that $\beta_{\text{even}} = \beta_{\text{odd}}$ at a frequency of 27.5 GHz. We have solved for both the magnetized and unmagnetized normal modes of the structure, using an $H$-field formulation of the FEM [8], [9]. The unmagnetized modes are used as input modes in the calculation of the nonreciprocal power transfer. Mazur had designed his FCL to be 14.3 mm in length. Our numerical results for $\ell = 14.3$ mm are shown in Fig. 4. Agreement with [4, Fig. 7] is good in terms of insertion loss, but less so for isolation. Our normal-mode theory shows that the optimum operation point is at $f \simeq 23.25$ GHz, which is significantly different from 27.5 GHz predicted by the coupled-mode theory.

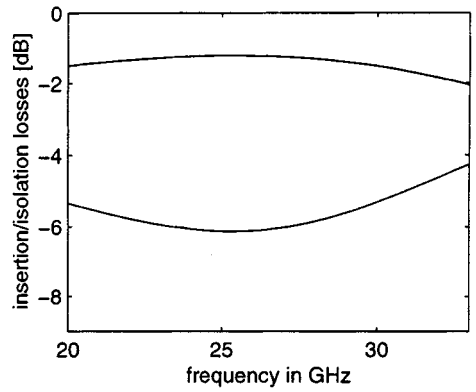


Fig. 4. Computed insertion loss and isolation of the FCL used in Mazur's experiment: $\ell = 14.3$ mm. Structural details are in the text.

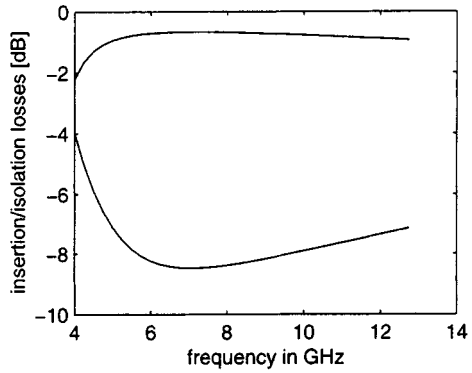


Fig. 5. Computed insertion loss and isolation of the FCL used in the Teoh *et al.* experiment. Structural details are in the text.

Consequently, the recommended length $\ell = 27.9$ mm of the FCL is different from that used in Mazur's experiment. Also, it should be noted that the maximum value of $(w_s/w)$ is only 0.6862, significantly smaller than the desired value of one.

The return loss estimated from (28) is lower than that measured by Mazur. The calculations on both the return and isolation losses may be improved if the reflections at the T-junction and at other interfaces of the distributed circulator are included.

The second numerical experiment is on the comparison of the new normal-mode optimum operation condition to the old condition of [3], [5], and [8]. The FCL structure is shown in Fig. 2, where region II has a thickness of 1.5748 mm and dielectric constant of $\varepsilon_d = 10.2$, region I consists of two layers, with the first layer immediately above the coupled striplines a 1.5-mm ferrite, which has a saturation magnetization $M_s = 111$ kA/m, $H_0 = 0$ A/m, and dielectric constant $\varepsilon_f = 11.7$. The region above the ferrite is air. Other dimensions in millimeters are $q = s = 0.75$, $d_1 = 6.4252$, $d_2 = 1.5748$, and $a = 8$ (data follows that of Teoh and Davis [5], [8]). Again, the eigenmodes of the unmagnetized FCL are used as input. The results on insertion and isolation losses for an even input for $\ell = 62$ mm are shown in Fig. 5. The Teoh *et al.* experimental result [5] contains some spurious signals, which may be due to unwanted reflections at discontinuities in their device. If we ignore these and consider the general behavior, the overall envelope of [5, Fig. 12] looks rather like Fig. 5.

The maximum value of $|(w_s/w)|$ for both even- and odd-mode input occurs at $f = 6.75$ GHz, quite close to 6.98 GHz, the value obtained in [3] by inspecting the phases $\phi_1$ and $\phi_2$. This means that at the optimum operation point, phase does approximately obey the rule of $\phi_{1,2} = \pm 90°$ ($\phi_{1,2} = \pm 109.7°$ in [5]). The length of the FCL found by the old normal-mode theory $\ell = 60.53$ mm (modified to 62 mm by consideration of impedance) is also close to $\ell = 57.6$ mm predicted by the new normal-mode theory. However, as with the coupled-mode theory, this old normal-mode theory does not have an assessment for the performance of the FCL at its optimum operation point, and perfect power transfer (equivalent to $|(w_s/w)| = 1$) is assumed. It is revealed in the new normal-mode calculation that the maximum power transfer factor is 0.72. This modest power transfer factor at the optimum operation point may be responsible for the poor performance of Teoh *et al.*'s experiment [5]. Also, there is an uncertainty in the old normal-mode theory. As mentioned before, the value of phase depends not only the position of the reference points, but also on the type of fields used in the calculation. Teoh *et al.* used the phase of the vertical-component of the $\mathbf{E}$ field vectors in the region immediately beneath each strip to get the result. Such uncertainty is avoided in the new theory.

The new normal-mode approach requires us to specify an input mode (odd or even) so that an isotropic input section for the magnetized FCL is needed. In the above numerical examples, we used the unmagnetized FCL as the input section, but it should be borne in mind that other waveguides can also be used as input sections. The need for an isotropic input section increases the computing time because eigenmodes of both the input and magnetized FCL sections need to be calculated. However, the magnetized FCL is found to perform quite differently when it is joined to different input sections. This fact suggests that the inclusion of a properly matched input section is essential. It seems that analyzing the magnetized FCL alone is not sufficient for the study of distributed circulators.

## IV. Numerical Results—New Structures

A good FCL should have large $|(w_s/w)|_{\max}$ broad bandwidth and short total length. It should also be compatible with the network in which it is embedded. Since stripline and microstrip line are the two most commonly used planar transmission lines, FCL's using these lines will be the focus for the remainder of this paper.

After some computer experiments it was found that the following microstrip FCL gave a satisfactory performance. This is by no means the most optimal structure, but it is one that gives a reasonably good $|(w_s/w)|_{\max}$ and a sufficiently short total length $\ell$. With the cross section of the microstrip FCL, as shown in Fig. 2, the structure has $d_1 = d_2 = 1.5$ mm, $q = 0.75$ mm, $s = 1.125$ mm, and $a = 2(q + s)$. Region I is air and region II is a ferrite with saturation magnetization $M_s = 239$ kA/m and dielectric constant $\varepsilon_f = 16$.[1] The isotropic input section has the same structure and dimensions as the FCL section, except that the ferrite medium is replaced by a material with dielectric

[1]Trans-Tech TT72-3005 Lithium ferrite, Trans-Tech SMAT-10 dielectric, Trans-Tech Inc., Adamstown, MD.

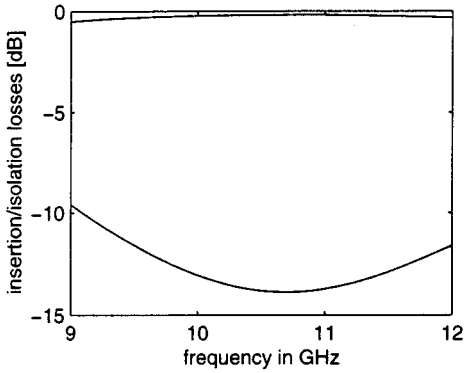


Fig. 6. Computed insertion loss and isolation of an FCL using microstrip lines. Structural details are in the text.

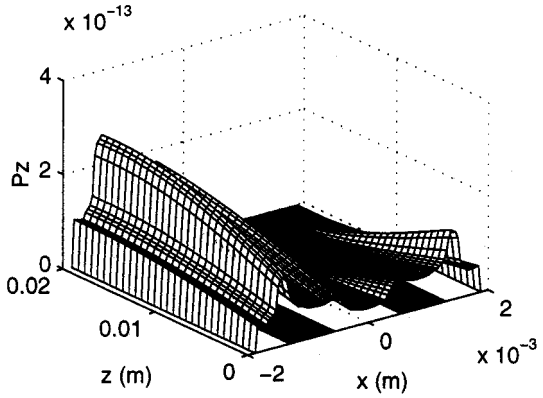


Fig. 7. Behavior of the microstrip FCL using even input. The shaded areas on the ground plane represent the two coupled microstrips. Magnetization is in the $z$-direction.

constant $\varepsilon_d = 10$.[1] Solving for the $\mathbf{H}$ field, with 440 edge elements, the power transfer factor $|(w_s/w)|$ and required length $L$ are calculated. The maximum value of $|(w_s/w)|$ is 0.918 at a frequency of 10.7 GHz, with required length of $L = 24.45$ mm. This is a larger value of $|(w_s/w)|$ than was achievable by the structures suggested by [4] and [5]. Assuming the T-junction is completely matched with the magnetized FCL, and using $\ell = L = 24.45$ mm in (26) and (27), the power transfer factor was converted into insertion loss and isolation and the results over a frequency range of 9.0 to 12.0 GHz are shown in Fig. 6. An insertion loss of about 0.18 dB and isolation of about 13.87 dB is achieved at the frequency of 10.7 GHz. The insertion loss is less than 0.5 dB, and the isolation is greater than 10 dB, at the band edges.

For confirmation, the $\mathbf{E}$ field has also been computed with the same number of elements. The calculated power transfer factor $|(w_s/w)|$ is about 0.914 at 10.7 GHz, and the required length $L$ at this frequency is 24.11 mm; both are close to what was obtained from the $H$-field calculation. These differences reduce when the number of elements used in the field calculation increases. The $z$-component of the power flow density $P_z = \int S_z\, dy$ at 10.7 GHz is plotted in Figs. 7 and 8 for an even- and an odd-input, respectively, under a $H_0\hat{z}$ magnetization. The power flow plots for a $-H_0\hat{z}$ magnetization showed that the direction of power transfer is reversed, but otherwise, they are mirror images of Figs. 7 and 8 are not shown here. These plots

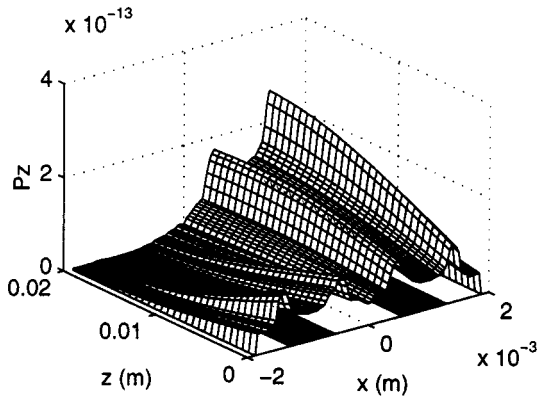


Fig. 8. Behavior of the microstrip FCL using odd input. The shaded areas on the ground plane represent the two coupled microstrips. Magnetization is in the $z$-direction.

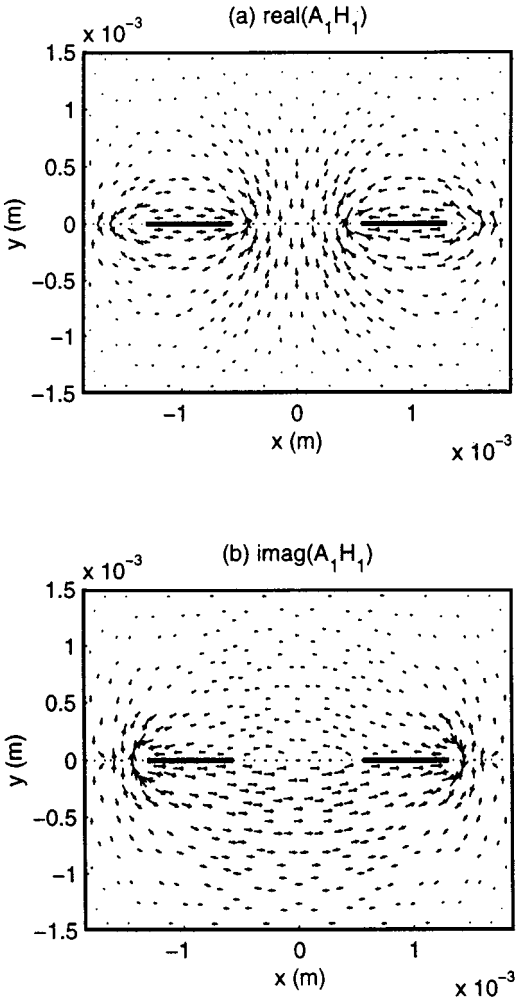


Fig. 9. Field plots of $A_1\mathbf{H}_1$ for $H_0\hat{z}$ magnetization.

are reminiscent of Fig. 3 (and demonstrate that the performance of the magnetized FCL is indeed nonreciprocal). It is controlled by the input condition (even or odd) and by the direction of magnetization. The imperfect behavior of this FCL is clearly evident because it can be seen that there is a small amount of power that is not transferred at the end of the coupled lines, as predicted.

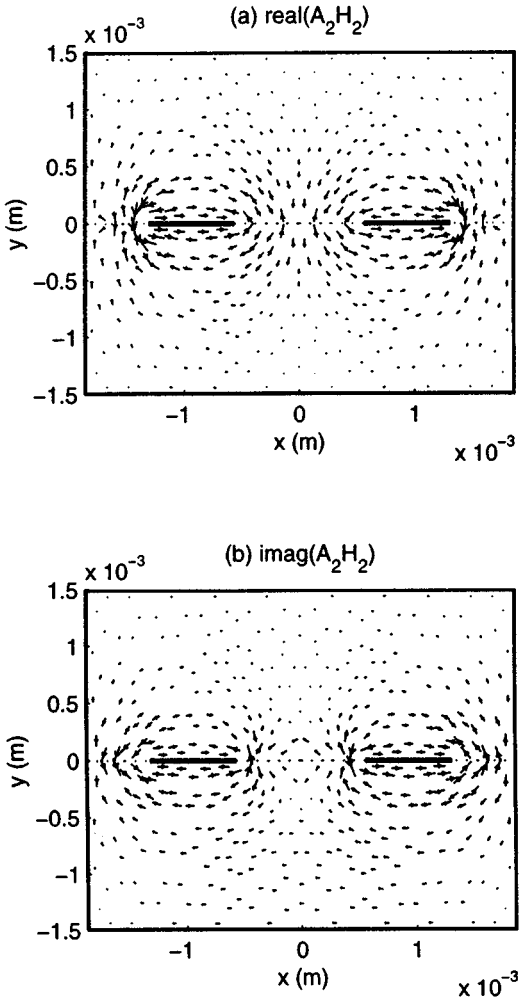


Fig. 10. Field plots of $A_2\mathbf{H}_2$ for $H_0\hat{z}$ magnetization.

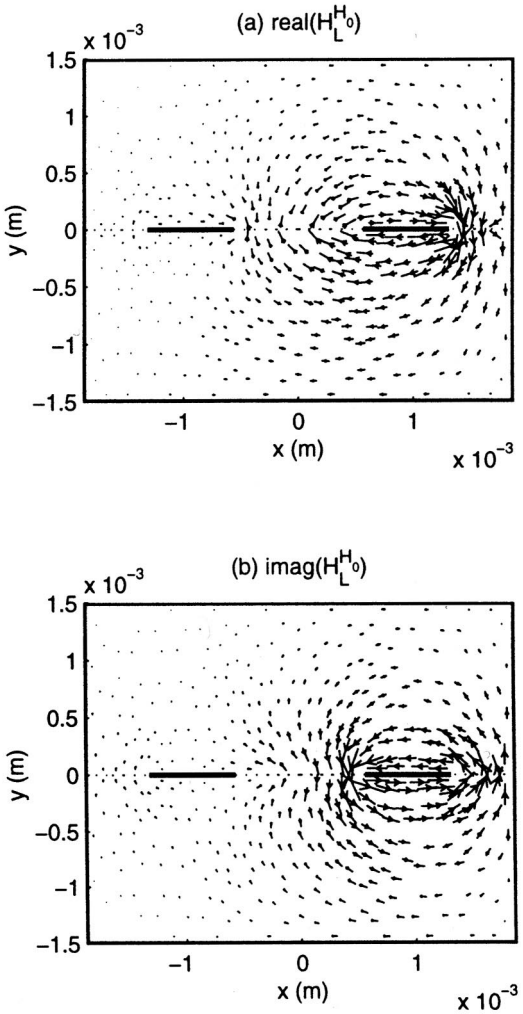


Fig. 11. Plots of $\mathbf{H}_L^{H_0}$. Definition details are in the text.

To see how the nonreciprocal behavior is achieved for the magnetized FCL, we reexamined the decomposition coefficients $A_1$, $A_2$, and the eigenmodes $\mathbf{H}_1$ and $\mathbf{H}_2$ to obtain

$$\mathbf{H}(z) = A_1\mathbf{H}_1 e^{-j\beta_1 z} + A_2\mathbf{H}_2 e^{-j\beta_2 z}. \tag{29}$$

Figs. 9 and 10 show $A_1\mathbf{H}_1 = A_1[H_{1x}\hat{x} + H_{1y}\hat{y} + H_{1z}\hat{z}]$ and $A_2\mathbf{H}_2 = A_2[H_{2x}\hat{x} + H_{2y}\hat{y} + H_{2z}\hat{z}]$ for an odd input when the FCL is magnetized in the $z$-direction $(H_0\hat{z})$. The field vector arrow used in these plots is defined as follows: direction and total length represents the transverse component of the field $H_t\hat{v} = H_x\hat{x} + H_y\hat{y}$, while the position of the tip of the arrowhead is determined by the ratio $(H_z/|H_t|)$. The field pattern at $z = 0$ for this $H_0\hat{z}$ magnetization is $\mathbf{H}^{H_0}(z = 0) = A_1\mathbf{H}_1 + A_2\mathbf{H}_2$, which can be obtained by directly adding up Figs. 9 and 10. It is seen that an approximately even $x$ distribution of power occurs.

At $z = L = (\pi/2)(1/|\beta_1 - \beta_2|)$, an extra phase of $-(\pi/2)$ is added to the first mode relative to the second mode; the role of its real and imaginary parts is, therefore, exchanged. The field pattern at $z = L$ is given by $\mathbf{H}^{H_0}(z = L) = \mathbf{H}_L^{H_0} e^{-j\beta_2 L}$, where

$$\begin{aligned}\mathrm{Re}\left(\mathbf{H}_L^{H_0}\right) &= +\mathrm{Im}(A_1\mathbf{H}_1) + \mathrm{Re}(A_2\mathbf{H}_2)\\ \mathrm{Im}\left(\mathbf{H}_L^{H_0}\right) &= -\mathrm{Re}(A_1\mathbf{H}_1) + \mathrm{Im}(A_2\mathbf{H}_2).\end{aligned} \tag{30}$$

The resulted fields have a big peak in the $x > 0$ side and a small peak in the $x < 0$ side, as shown in Fig. 11. Consequently, most of the input power is switched to the right line. Manipulations on the electric-field components $\mathbf{E}_1$, $\mathbf{E}_2$ give the same answer.

When the direction of magnetization is changed from $H_0\hat{z}$ to $-H_0\hat{z}$ for the same input, it can be seen from Tables I and II that $A_1[H_{1x}\hat{x} + H_{1y}\hat{y} + H_{1z}\hat{z}]$ and $A_2[H_{2x}\hat{x} + H_{2y}\hat{y} + H_{2z}\hat{z}]$, respectively, become $A_1^*[H_{1x}^*\hat{x} + H_{1y}^*\hat{y} - H_{1z}^*\hat{z}]e^{j(2\psi_o - \theta_o)}$ and $A_2^*[H_{2x}^*\hat{x} + H_{2y}^*\hat{y} - H_{2z}^*\hat{z}]e^{j(2\psi_o - \theta_o)}$, where $e^{j(2\psi_o - \theta_o)}$ is a common phase factor that is arbitrary and can be set to zero. The field at $z = 0$ for this magnetization is

$$\begin{aligned}\mathbf{H}^{-H_0}(z = 0) = {} & A_1^*\left[H_{1x}^*\hat{x} + H_{1y}^*\hat{y} - H_{1z}^*\hat{z}\right]e^{j(2\psi_o - \theta_o)}\\ & + A_2^*\left[H_{2x}^*\hat{x} + H_{2y}^*\hat{y} - H_{2z}^*\hat{z}\right]e^{j(2\psi_o - \theta_o)}\end{aligned} \tag{31}$$

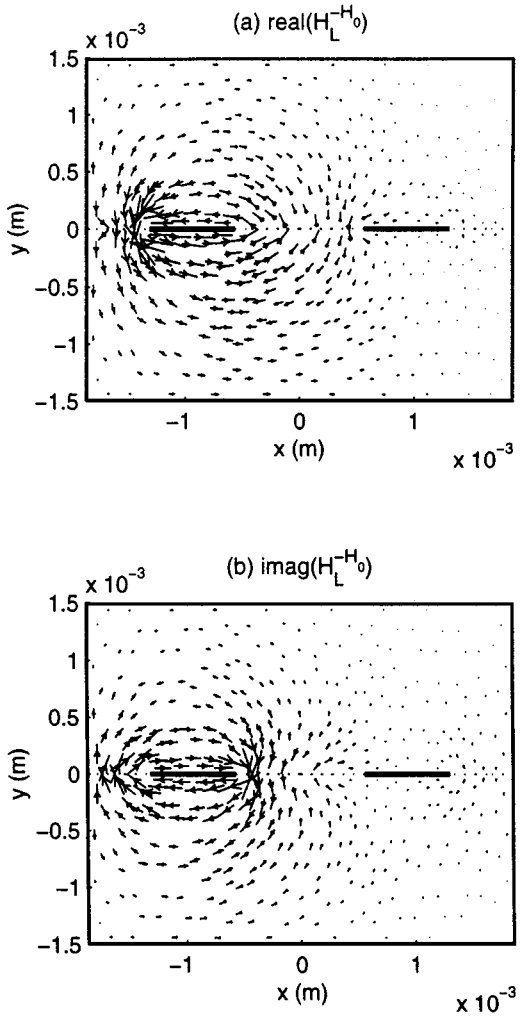


Fig. 12. Plots of $\mathbf{H}_L^{-H_0}$. Definition details are in the text.

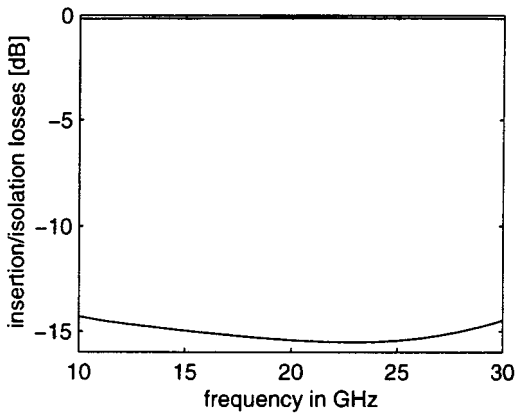


Fig. 13. Computed insertion loss and isolation of the FCL using striplines. Structural details are in the text.

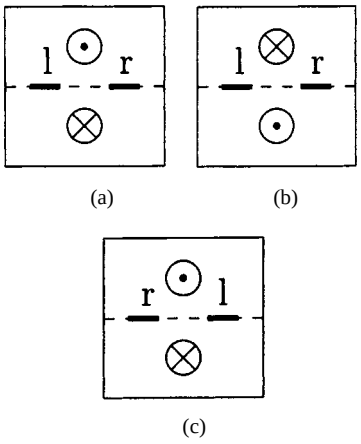


Fig. 14. Cross section of the dually magnetized symmetrical FCL.

which still produces an even power distribution between the two coupled lines. However, at $z = L$, the magnetic field becomes $\mathbf{H}^{-H_0}(z = L) = \mathbf{H}_L^{-H_0} e^{-j\beta_2 L} e^{j(2\psi_o - \theta_o)}$, where

$$\mathrm{Re}\left(\mathbf{H}_L^{-H_0}\right) = -\mathrm{Im}\Big(A_1[H_{1x}\hat{x} + H_{1y}\hat{y} - H_{1z}\hat{z}]\Big) + \mathrm{Re}\Big(A_2[H_{2x}\hat{x} + H_{2y}\hat{y} - H_{2z}\hat{z}]\Big) \quad (32)$$

$$\mathrm{Im}\Big(\mathbf{H}_L^{-H_0}\Big) = -\mathrm{Re}\Big(A_1[H_{1x}\hat{x} + H_{1y}\hat{y} - H_{1z}\hat{z}]\Big) - \mathrm{Im}\Big(A_2[H_{2x}\hat{x} + H_{2y}\hat{y} - H_{2z}\hat{z}]\Big). \quad (33)$$

The resulted fields have a big peak in the $x < 0$ side, as shown in Fig. 12. This means most of the input power is switched to the left line in this $-H_0\hat{z}$ magnetization, i.e., opposite to the case of $H_0\hat{z}$ magnetization.

It is clearly seen that when the direction of the magnetization on the FCL is reversed, the effects on the decomposition coefficients $A_1$ $A_2$ and the effects on the eigenmodes $[\mathbf{E}_1(x,y), \mathbf{H}_1(x,y)]$, $[\mathbf{E}_2(x,y), \mathbf{H}_2(x,y)]$ worked together and produced the nonreciprocal performance of the FCL. It also becomes apparent that the incomplete power transfer between the two coupled lines is due to the different $x$, $y$ dependence of the eigenmodes, so that any component, e.g., $A_1H_{1x}$ and $A_2H_{2x}$, do not completely cancel each other everywhere on the left-hand side (right-hand side) half of the structure for $H_0\hat{z}$ $(-H_0\hat{z})$ magnetization. This incomplete cancellation of the eigenmodes is not special for magnetized FCL. It is an intrinsic characteristic of any coupled lines. Only in an idealized situation will this ratio become one [11].

A better result can be obtained from an FCL built using a stripline-type structure rather than microstrip. The cross section of this stripline FCL is as shown in Fig. 2, with $d_1 = d_2 = 0.5$ mm, $q = s = 0.5$ mm, and $a = 2(q + s)$. Region I has a dielectric constant $\varepsilon_d = 10.2$. Region II is ferrite with a saturation magnetization $M_s = 111$ kA/m and dielectric constant $\varepsilon_f = 11.7$. The unmagnetized "stripline" FCL is used as the input section. The power transfer factor $|(w_s/w)|$ and the required length $L$ for an even input are calculated and the results are converted into insertion loss and isolation for a $\ell = 101.2$ mm stripline FCL over the frequency range of 10–30 GHz, as shown in Fig. 13. An insertion loss of 0.12 dB and isolation of 15.5 dB are achieved at 23 GHz, and the insertion loss and isolation are better than 0.17 and 14 dB, respectively, at the band edges. It is noted that both the performance and bandwidth of this stripline FCL are better than those of the microstrip FCL. Unfortunately, the length $\ell$ of the resulted FCL is larger.

One way to reduce $\ell$ is to use two ferrites: replacing the dielectric material (region I) with the same ferrite as region II, then magnetizing them in opposite directions. The outcome is a special type of "dual" FCL, as shown in Fig. 14. Such an FCL has also other advantages. For example, its $(w_c/w)$ and $(\triangle w/w)$ are exactly zero for any frequency.

## V. Conclusion

A rigorous full-wave normal-mode treatment of the magnetized FCL has been presented for use in the design of novel circulators. The eigenmode solution of an FCL magnetized longitudinally in the $z$-direction was found to bear a simple relationship to the eigenmode solution of the same FCL when magnetized in the opposite direction. By reversing the direction of magnetization, the change in the decomposition coefficients of the same input wave into the eigenmodes of the $\pm z$ magnetized FCL is studied. The nonreciprocal effect demonstrated by the magnetized FCL is explained in terms of the changes in the eigenmodes and in the decomposation coefficients.

A new optimum operation condition was constructed from the Poynting vector. This new condition takes into account all available information such as the propagation constants, the amplitude, and the phase of the guided waves, including both $\mathbf{E}$ and $\mathbf{H}$ components. The new condition not only gives a more accurate description of a given FCL versus frequency than the old conditions, it also enables the performance of different FCL structures to be assessed so that an overall best FCL can be identified.

Detailed theoretical comparisons have been made with experimental circulator results in the literature, and new microstrip and stripline structures have been described with promising predicted performance.

## Appendix A
## Changes in the Guided Modal Field Patterns When the Direction of the Magnetization $H_0\hat{z}$ Is Reversed

$\mathbf{H}$ and $\mathbf{E}$ can be separated into transverse and longitudinal components

$$\mathbf{H} = (H_t\hat{v} + H_z\hat{z})e^{-j\beta z} \quad \mathbf{E} = (E_t\hat{u} + E_z\hat{z})e^{-j\beta z} \tag{34}$$

where $\hat{z}$ is the unit vector in the longitudinal direction, and $\hat{u}$ and $\hat{v}$ are unit vectors in the direction of the transverse components of $\mathbf{E}$ and $\mathbf{H}$. Since the $z$ dependence of the fields is already made explicit by factoring out $e^{-j\beta z}$, $\nabla$ can also be split into a transverse component $\nabla_t$ and a longitudinal component $(\partial/\partial z)\hat{z} = -j\beta\hat{z}$. Substituting (34) into (1) and (2), we get [12] for the longitudinal components

$$\left(\mu\nabla_t^2 + \frac{\omega^2}{c^2}\varepsilon\mu - \beta^2\right)H_z + j\omega\varepsilon\varepsilon_0\kappa\beta E_z = 0 \tag{35}$$

$$\left(\mu\nabla_t^2 + \frac{\omega^2}{c^2}\varepsilon\mu^2 - \mu\beta^2\right)E_z - j\omega\mu_0\kappa\beta H_z - \frac{\omega^2}{c^2}\varepsilon\kappa^2 E_z = 0 \tag{36}$$

The transverse components $E_t$ and $H_t$ are related to $E_z$ and $H_z$ through

$$\left(\frac{\omega^2}{c^2}\varepsilon\mu - \beta^2\right)H_t\hat{v} - j\frac{\omega^2}{c^2}\varepsilon\kappa\hat{z}\times\hat{v}H_t + j\beta\nabla_t H_z + j\omega\varepsilon\varepsilon_0\hat{z}\times\nabla_t E_z = 0 \tag{37}$$

$$\left(\frac{\omega^2}{c^2}\varepsilon\mu - \beta^2\right)E_t\hat{u} - j\frac{\omega^2}{c^2}\varepsilon\kappa\hat{z}\times\hat{u}E_t + j\beta\nabla_t E_z - j\omega\mu\mu_0\hat{z}\times\nabla_t H_z + \omega\mu_0\kappa\nabla_t H_z = 0. \tag{38}$$

Equations (35)–(38) can be used to describe the behavior of the fields in the entire waveguide structure, provided that $\varepsilon$, $\mu$, and $\kappa$ are treated as functions of $x$ and $y$. The effect of reversing the magnetization $H_0\hat{z}$ is to change the sign of $\kappa$. Taking the complex conjugate of (35)–(38), reversing the sign of $\kappa$, and then comparing the result with (35)–(38), we find that if $\beta$ and $[E_t(x,y), E_z(x,y), H_t(x,y), H_z(x,y)]$ are the eigenvalue and eigenvector of an FCL with a magnetization of $H_0\hat{z}$, then $\beta$ and $[E_t^*(x,y), -E_z^*(x,y), H_t^*(x,y), -H_z^*(x,y)]e^{-j\theta}$ will be the eigenvalue and eigenvector of the same FCL with the opposite magnetization $(-H_0\hat{z})$, where $\theta$, independent of $x$, $y$, and $z$, is an arbitrary phase shift. The propagation constant $\beta$ is not changed in this process, which confirms the bidirectionality theorem. The change in the modal profile will enable us to predict the performance of the magnetized FCL when $H_0\hat{z}$ is reversed.

## Appendix B
## Power Flow in Dually Magnetized Symmetrical FCL

Unlike a symmetrical dielectric waveguide, in an FCL magnetized in the $z$-direction, the power flow on the right-hand side of the waveguide is generally not equal to the power flow on the left-hand side of the waveguide. A specially magnetized FCL is shown in Fig. 14(a), in which both media above and below the coupled lines are identical ferrites with the same thickness and width, but magnetized in opposite $(\pm z)$-directions. The two lines, $r$ and $l$, are also the same and are placed at $y = 0$ and symmetrical about $x = 0$ (see Fig. 2 for the coordinate system). For such a dually magnetized symmetrical FCL, we have

$$\mathrm{Re}(P_{iir}) = \mathrm{Re}(P_{iil}), \qquad i = 1, 2. \tag{39}$$

The proof of (39) is the following. If we assume

$$\mathrm{Re}(P_{iir})_a > \mathrm{Re}(P_{iil})_a \tag{40}$$

for the FCL structure shown in Fig. 14(a), then, by reversing the direction of the magnetization in both ferrites, we get a structure that looks like Fig. 14(b). Using (18), we get

$$(P_{iir})_b = (P_{iir}^*)_a \quad (P_{iil})_b = (P_{iil}^*)_a. \tag{41}$$

Equation (40), therefore, becomes

$$\mathrm{Re}(P_{iir})_b > \mathrm{Re}(P_{iil})_b. \tag{42}$$

If the FCL in Fig. 14(b) is now rotated by 180° around the $z$-axis, we get to Fig. 14(c), and

$$(P_{iir})_c = (P_{iir})_b \quad (P_{iil})_c = (P_{iil})_b. \tag{43}$$

The resulted configuration Fig. 14(c) is exactly the same as Fig. 14(a), except that "$r$" and "$l$" are defined in an opposite way, i.e.,

$$(P_{iir})_c = (P_{iil})_a \quad (P_{iil})_c = (P_{iir})_a. \tag{44}$$

Using (44) and (43) in (42), we get

$$\mathrm{Re}(P_{iil})_a > \mathrm{Re}(P_{iir})_a \tag{45}$$

which violates (40). The opposite of (40) cannot be true either, we have, therefore, proven $\mathrm{Re}(P_{iir}) = \mathrm{Re}(P_{iil})$.

In such a dually magnetized symmetrical FCL, it can be proven that, for a pure even or pure odd input, that

$$w_{cr} = w_{cl} = 0 \tag{46}$$

where

$$w_{cr} = \frac{1}{2}\,\mathrm{Re}\Big(A_1 A_2^* P_{12r} + A_1^* A_2 P_{21r}\Big)$$
$$w_{cl} = \frac{1}{2}\,\mathrm{Re}\Big(A_1 A_2^* P_{12l} + A_1^* A_2 P_{21l}\Big). \tag{47}$$

If we start by assuming

$$w_{cr}|_a > w_{cl}|_a \tag{48}$$

for the structure of Fig. 14(a), and reversing the direction of magnetization ($H_0\hat{z} \rightarrow -H_0\hat{z}$), we come to Fig. 14(b), and it follows from the relationships in (20) that $w_{cr}|_b = w_{cr}|_a$ and $w_{cl}|_b = w_{cl}|_a$. Fig. 14(b) is then rotated ($r \rightarrow l, l \rightarrow r$), and the structure becomes Fig. 14(c). Since Fig. 14(a) is the same as Fig. 14(c), we have

$$w_{cl}|_b = w_{cl}|_c > w_{cr}|_c = w_{cr}|_b \tag{49}$$

therefore,

$$w_{cl}|_a > w_{cr}|_a \tag{50}$$

which disagrees with the initial assumption (48). It can also be proven that the opposite of (48) is not true either, thus, $w_{cr} = w_{cl}$. However, $w_{cr} + w_{cl} = (1/2)\,\mathrm{Re}(A_1 A_2^* P_{12} + A_1^* A_2 P_{21}) = 0$, according to the orthogonality of the guided modes. Therefore, $w_{cr} = w_{cl} = 0$ is the only possible answer for an FCL of this special type.

It follows from (14) that $W_r(z = 0) = w_{0r} + w_{cr}$ and $W_l(z = 0) = w_{0l} + w_{cl}$, where

$$w_{0r} = \frac{|A_1|^2}{2}\,\mathrm{Re}(P_{11r}) + \frac{|A_2|^2}{2}\,\mathrm{Re}(P_{22r})$$
$$w_{0l} = \frac{|A_1|^2}{2}\,\mathrm{Re}(P_{11l}) + \frac{|A_2|^2}{2}\,\mathrm{Re}(P_{22l}). \tag{51}$$

Using (39) in (51) gives $w_{0r} = w_{0l}$, thus, (46) actually means that $W_r(z = 0) = W_l(z = 0)$, i.e., power is initially evenly launched into the coupled lines. It should be noted that the above proof is valid only for pure even or pure odd input. If the input is a mixture of even and odd modes, the relationships in (20) do not exist and we then cannot prove or disprove (48). Launching all or most of the power into one of the lines is a common practice in reality.

## REFERENCES


[1] L. E. Davis and D. B. Sillars, "Millimetric nonreciprocal coupled-slot finline components," *IEEE Trans. Microwave Theory Tech.*, vol. MTT-34, pp. 804–808, July 1986.

[2] J. Mazur and M. Mrozowski, "On the mode coupling in longitudinally magnetized wave-guiding structures," *IEEE Trans. Microwave Theory Tech.*, vol. 37, pp. 159–165, Jan. 1989.

[3] C. S. Teoh and L. E. Davis, "Normal-mode analysis of ferrite-coupled-lines using microstrips or slotlines," *IEEE Trans. Microwave Theory Tech.*, vol. 43, pp. 2991–2998, Dec. 1995.

[4] J. Mazur, "Millimeter-wave three-port finline circulator using distributed coupling effect," *IEEE Trans. Microwave Theory Tech.*, vol. 41, pp. 1067–1070, June 1993.

[5] C. S. Teoh and L. E. Davis, "Optimized design of novel microstrip FCL circulators," unpublished.

[6] P. R. McIsaac, "Bidirectionality in gyrotropic waveguides," *IEEE Trans. Microwave Theory Tech.*, vol. MTT-24, pp. 223–226, Apr. 1976.

[7] A. Konrad, "Vector variational formulation of electromagnetic fields in anisotropic media," *IEEE Trans. Microwave Theory Tech.*, vol. MTT-24, pp. 553–559, Sept. 1976.

[8] C. S. Teoh, "Ferrite-coupled planar microwave devices," Ph.D. dissertation, Dept. Elect. Eng. Electron., UMIST, Manchester, U.K., 1996.

[9] M. Koshiba and K. Inoue, "Simple and efficient finite-element analysis of microwave and optical waveguides," *IEEE Trans. Microwave Theory Tech.*, vol. 40, pp. 371–377, Feb. 1992.

[10] D. M. Pozar, *Microwave Engineering*. Reading, MA: Addison-Wesley, 1990, pp. 251–259.

[11] P. K. Ikalainen and G. L. Matthaei, "Wide-band, forward coupling microstrip hybrids with high directionality," *IEEE Trans. Microwave Theory Tech.*, vol. MTT-35, pp. 719–725, Aug. 1987.

[12] R. A. Waldron, "Electromagnetic wave propagation in cylindrical waveguides containing gyromagnetic media," *J. British Inst. Radio Eng.*, vol. 18, pp. 597–612, Oct. 1958.



**Kang Xie** (M'98), photograph and biography not available at time of publication.

**Lionel E. Davis** (SM'64–F'95), photograph and biography not available at time of publication.